REMOTELY SENSED CAVE DETECTION ON EARTH AND MARS. C. A. Drost[1], J. J. Wynne[1], M. G. Chapman[1], J. S. Kargel[2], T. N. Titus[1], and R. S. Toomey[3] ([1]US Geological Survey, 2255 N. Gemini Drive, Flagstaff, AZ 86001, cdrost@usgs.gov; [2]Dept. of Hydrology, U. of A., Tucson, AZ 85721; [3]Western Kentucky University, Bowling Green, KY 42101-1066).

Introduction: This is a progress report on a study evaluating the use of thermal remote sensing to identify and characterize caves on Earth and Mars. Methods used include: (1) assessment of geologic formations and surface conditions on Mars that may be associated with the formation and occurrence of caves; (2) selection of large Earth-analog caves detectable using remote sensing instruments; (3) development of a predictive model for the thermal signal generated by caves; (4) terrestrial ground-based instrument measurements to evaluate general conditions and requirements for remote sensing of caves; (5) remote sensing measurements of terrestrial caves from intermediate-level platform (helicopter or fixed-wing aircraft); and (6) extrapolation of Earth-based data to instrument requirements for detecting caves on Mars.

Cave Detection on Earth: The physical basis for resolving a "detectable signal" requires identification of signal magnitude, radiant energy, the variation of the signal over time, and the interdependence of the signal on other natural phenomena [1]. A 24-hour dataset collected in late-September from Grand Wash Cave in northern Arizona shows a temperature difference between 5 to 8° F between the cave entrance and ambient temperature (Fig. 1). Thermograms from from Carlsbad Caverns, New Mexico ([2]; Fig. 2) demonstrate a 10° to 30° F temperature difference between the internal surface of the cave walls and the surface of the external rock. Additional work will add to and refine our understanding of these phenomena, in relation to planned analysis of thermal remote sensing data for detecting caves.

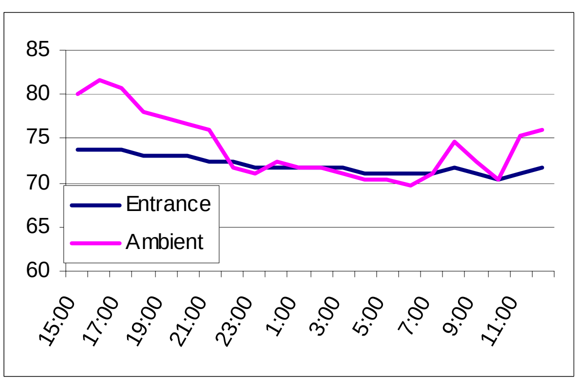

Figure 1. Ambient and cave entrance temperatures from Grand Wash Cave, Arizona.

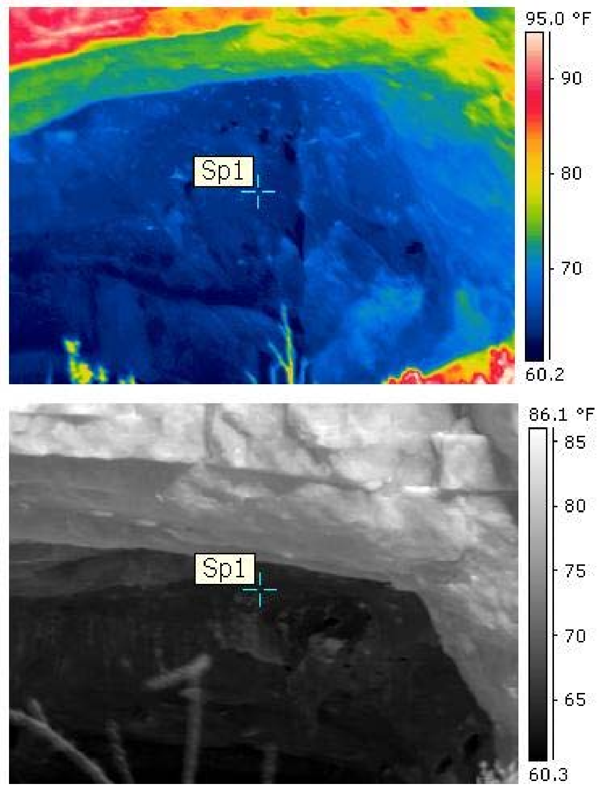

Figure 2. Thermograms of Carlsbad Caverns main entrance, New Mexico. Imagery was captured on April 9, 2005 using a FLIR Therma CAM™ B20 HSV thermographic camera [2]; 'Sp1' denotes reference point.

Subterranean Features on Mars: On Mars, subterranean features are likely to be present as (1) karst caves in hydrated salts and thermokarstic caves in ice-rich permafrost and debris-covered glaciers and (2) areas of collapsed lava tubes associated with lava channels and plains. A thermokarst area is located within Utopia Planitia (Fig. 3); MOC images of the polygonal cracks show numerous voids that may be possible caverns [3]. Lava tubes with possibly detectible openings/caves are likely to be best preserved in young materials. Using GIS, we relegated this search to Amazonian-aged volcanic units shown on the digital global geologic maps of Mars [4, 5]. Recently, a high-resolution search of MOC images noted that lava tubes and channels on Olympus Mons are found on the flanks between slopes of 0° to 17° [6]. Using MOLA, we removed from the search area all slopes in the Amazonian lava plains greater than 17°. Large amounts of surface dust and aeolian materials could infill Martian caves and deter detection; therefore we further eliminated all areas that were indicated by TES to have a surface composition of more than 50 percent dust [7, 8]. Six remaining areas were designated by this search that included (1) south Daedalia Planum, (2) Sinai and Solis Planum, (3) Acidalia Planitia, (4) the south rim of Hellas Planitia, (5) Hadriaca Patera, and (6) Hesperia Planum (Fig. 3). GIS indicates that these areas are visually covered by at least 2,076 MOC narrow angle (NA) images (Fig. 3). The TES data resolution is very coarse. For example, a lava tube site within TES designated dust free area 2 (Sinai Planum) shows a lot of cover at MOC scale (Fig. 4). Therefore our next step will be to narrow down our search within these 6 areas to only MOC NA covered locales of exposed bedrock, using GIS overlays of THEMIS daytime infrared & nighttime infrared data. Once these bedrock areas are located, we will begin a manual search of the remaining MOC NA images.

Conclusion: Work on this project is proceeding in three major areas: 1) detailed on-site measurements of thermal properties of terrestrial caves, together with thermal imaging of cave-bearing formations on earth; 2) development of computer models that characterize thermal properties of caves; and 3) delineation of areas on the surface of Mars likely to contain lava tube caves, and computerized and visual scrutiny of these areas for caves and cave-like structures. Synthesis of this information should lead to better understanding of the character and likely location of caves on the surface of Mars, and improved capabilities for identifying and characterizing such caves.

References: [1] Rinker J. N. (1975) *Photogram. Eng. Remote Sensing* 41, 1391-1400; [2] Thompson J. and M. Murray (2005) Experimental research using thermography to locate heat signatures from caves, unpubl. report; [3] Kargel J. S. (2004) Mars, Springer, UK, p. 258-259; [4] Scott D. H., and K. L. Tanaka (1986) *U.S. Geol. Surv. Misc. Invest. Ser. Map* I-1802-A, 1:15,000,000 scale; [5] Greeley R. and J. E. Guest (1987) *U.S. Geol. Surv. Misc. Invest. Ser. Map* I-1802-B, 1:15,000,000 scale; [6] Parcheta C. (2005) AGU 2005 Fall Meeting, *Eos Trans. Suppl*., Abstract P23A-0179; [7] Bandfield J. L. and M. D. Smith (2003) *Icarus* 161, 47-65; [8] Bandfield et al. (2003) *Science* 301, 1084-1087.

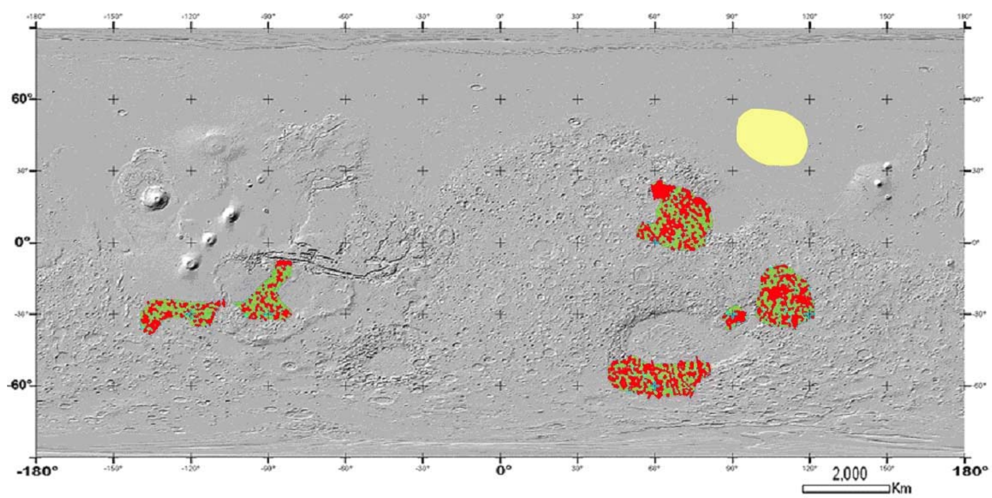

Figure 3: Yellow area denotes polygonal terrain and red color denotes MOC NA coverage (2,076 images) within six areas of Amazonian-aged volcanic plains having slopes < 17° and < 50% TES detected surface dust cover.

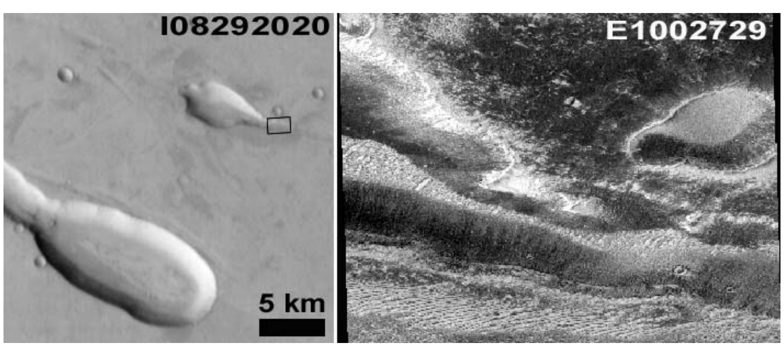

Figure 4: Sinai Planum THEMIS Infrared image of lava tubes on left (about long. -90° W. & lat. -8°); box denotes location of dusty MOC NA image on right. Scale bar shown on left.